25. A Comparison of Ductile and Fatigue Fractures

C. CRUSSARD, J. PLATEAU, R. TAMHANKAR, G. HENRY, and D. LAJEUNESSE

Institut de Recherches de la Sidérurgie
Saint-Germain-en-Laye, France

ABSTRACT

The relation between the fatigue strength and the tensile properties of steels of different hardness levels is examined. The endurance limit is found to correlate best with the ultimate tensile strength. Observations of tensile fracture and necking of round and of thin, flat specimens are reported. The results of electron microscope studies of the appearance of fibrous, shear, and fatigue fracture surfaces are described, and deductions pertaining to the mechanism of fracture are discussed. The correlation between endurance limit and ultimate tensile strength and the similarities found to exist between shear and fatigue rupture surfaces are associated with the magnitude of the local strain propagating in a narrow rupture zone.

Introduction

Frequent attempts have been made to find a relation between the fatigue limit of metals and some characteristic stress deduced from their tensile properties. Although at first glance it seems that the fatigue limit should be related to the *yield stress*, it is generally stated in classical text books on fatigue [1] that it varies from metal to metal as a function of *tensile strength*. This relation has been confirmed for a number of metals [2] by low-temperature tests.

From a statistical point of view, the number of samples tested by other workers is sometimes rather meager for a good correlation to be established, when due consideration is given to the scatter in fatigue as well as in tensile tests. The first part of this chapter will be devoted to an investigation of the relation between fatigue limit and tensile strength in

several ferritic steels: One series of tests was made on a large number of specimens representing a wide range of hardness; other similar tests were conducted on one of these steels at various temperatures, especially in the blue-brittleness range. These tests have enabled a study of the influence of hardness or temperature on the appearance of the tensile fracture.

As will be seen later, this part of the study confirms the relation between fatigue limit and ultimate tensile stress. The possibility of similar modes of fracture in the tensile and in the fatigue tests was therefore considered. An interesting approach to this problem seemed to be a careful study of the appearance of fracture surfaces obtained in both modes of rupture. For that part of the study, use has been made of the new microfractographic technique that has proved so successful in the study of fracture.[3–5] This technique consists of examining, with the electron microscope, carbon replicas of the fracture surfaces, which are stripped either electrolytically or after immersion in a solution of bromine in alcohol.[6] The great depth of focus of the electron microscope permits observation of the fine details on fracture surfaces that are too irregularly contoured and wavy to be examined by optical microscopy.

The observations made in these two parts, macroscopic and microscopic, will also give very interesting information on the mechanism of ductile failure.

Mechanical Tests

Relation Between Fatigue Limit and Ultimate Tensile Stress

Unnotched specimens of several ferritic steels, the compositions of which are given in Table 1, have been annealed or heat-treated (quenched

TABLE 1. Chemical Compositions

%

Steel No.	C	Si	Mn	S	P	Ni	Cr	Mo
I	0.10	0.15	0.41	0.007	0.007	—	—	—
II	0.125	0.035	0.43	0.026	0.010	—	—	—
III	0.35	0.20	0.46	0.005	0.06	—	—	—
IV	0.38	0.13	0.50	0.02	0.017	—	—	—
V	0.75	0.35	0.42	0.005	0.09	—	—	—
VI	0.37	0.33	0.59	0.009	0.021	2.75	1.05	0.14
VII	0.41	0.20	0.66	0.001	0.025	—	1.07	0.18
VIII	0.43	0.28	0.52	0.008	0.020	4.75	1.8	0.53

and tempered or simply quenched) and tested in fatigue at room temperature (rotating bending-cantilever type or constant-moment type), 120 specimens being used to determine each endurance limit. Tensile

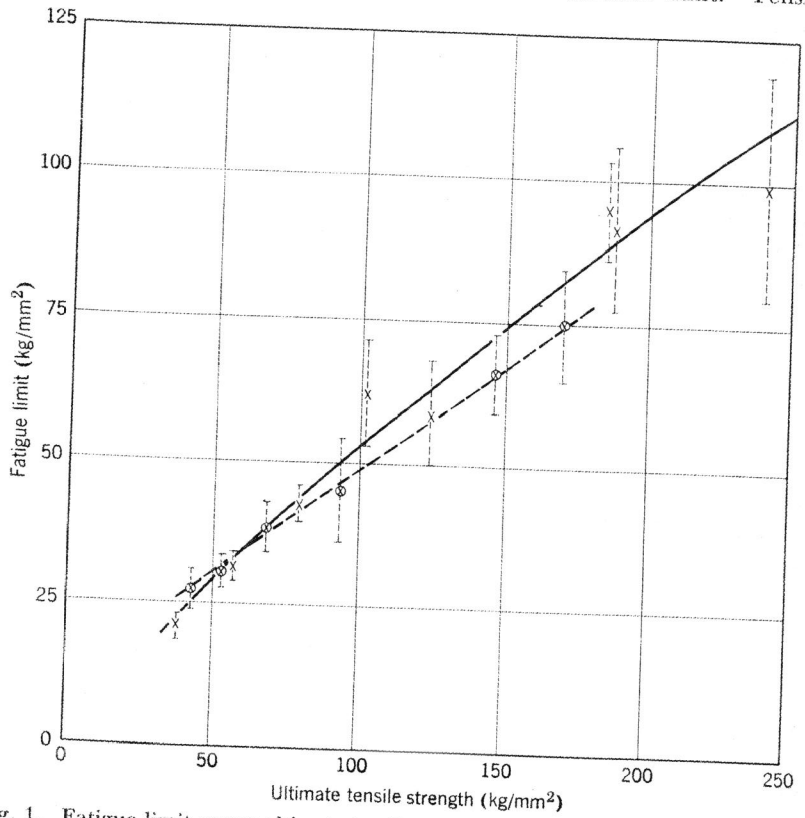

Fig. 1. Fatigue limit versus ultimate tensile strength. Scatter range is for the 5% to 95% interval. ⊗ specimens ground from fatigue test pieces, × normal tensile specimens.

tests have been performed either on test pieces ground from untested fatigue specimens or on normal tensile specimens treated in the same way as fatigue specimens. The results are plotted in Fig. 1, with the scatter range of each fatigue limit indicated. (The scatter ranges of ultimate tensile strength have not been shown, as they are small, about 2 to 3%.)

A distinction has been made between the points on the graph obtained from the two types of specimens;[3] the points with circles (specimens ground from fatigue test pieces) are well aligned on a straight line that does not pass through the origin, while the points representing normal tensile specimens show more scatter. All results considered, a good curve is obtained which is nearly a straight line bending towards the origin.

A plot of hardness or resistance to torsion versus endurance limit for specimens ground from fatigue test pieces does not give as good a straight line as Fig. 1. The reason for this will be discussed later.

For steel IV (Table 1) tested in the annealed state at temperatures between room temperature and 400°C, it is observed that the ratio F/R (F = fatigue limit, R = ultimate tensile strength) remains very constant (between 0.44 and 0.48), while F/Y (Y = yield stress) varies in much larger limits, going from 0.55 to 0.8. The values of F and R fall close to the curve of Fig. 1. At temperatures above 450°C, the relation does not hold, F/R increasing markedly.*

Tensile Fracture and Necking

In the preceding paragraph, we have confirmed the existence of a linear (almost proportional) relationship between endurance limit and ultimate tensile strength. As the endurance limit is a critical stress level for rupture (in fatigue), it might seem that it should be correlated with the rupture stress in tensile tests, that is, with the true stress in the fracture area at the time of rupture or, as it is also called, the *technical cohesion*. As a matter of fact, the ultimate tensile strength is more closely related to an instability in the balance between geometrical and strain-hardening factors than to some characteristic cohesive properties of the metal.

In order to investigate this point, it is interesting to observe how the appearance of tensile fracture varies with temperature or hardness level of the steel. Except for the very hard steels, these fractures are of the well-known "cup-and-cone" type, with a central fibrous† portion (the average orientation of which is normal to the axis) surrounded by a smoother conical surface corresponding to a "shear" fracture. It is well known that the rupture initiates in the central fibrous region and propagates toward the peripheral surface. An acoustical study [8] has proved that, in this central area, the propagation is rather slow, requiring of the order of about 20 to 50 millisec for samples of 3-mm diam.

For an as-rolled 0.10% carbon steel, the same cup-and-cone fracture is observed in tests at temperatures of up to 500°C. The central fibrous region has almost the same area at temperatures up to 400°C, while the area of cone fracture passes through a maximum at 200°C (Fig. 2). This means that at this temperature the percent reduction in area at rupture passes through a minimum. This temperature of 200°C also corresponds to a maximum of the ultimate tensile strength (Fig. 2) and lies in the "blue-brittle range."

The acoustical study [8] on smaller samples tested at 200°C proves that,

* Results obtained in the authors' laboratory by M. Weisz and R. Cazaud.[7]

† We use here Orowan's terminology.

in some samples where the fracture is almost entirely of the shear type (on a plane inclined to the axis), the propagation of the rupture is extremely rapid, its duration being smaller than 2 to 3 millisec. This is

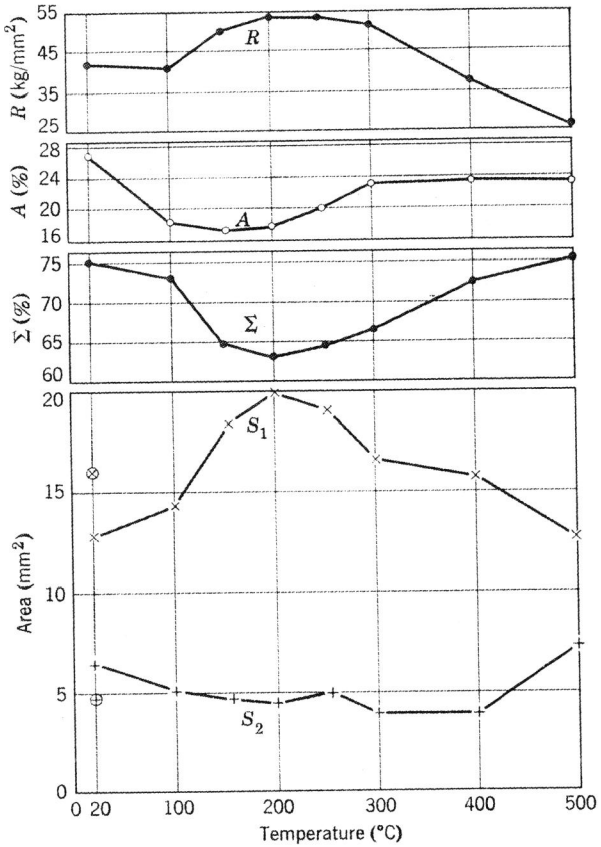

Fig. 2. Results of tensile tests at different temperatures for mild steel. R = ultimate tensile strength, A = elongation (%), Σ = reduction in area (%), S_1 = area of fracture surface, S_2 = area of bottom of the cups, ⊕⊗ = specimen deformed to 15% at 250°C, then broken in tension at 20°C.

of the order of the time of response of the acoustic and electronic device used in the experiment.

We can thus picture the mechanism of cup-and-cone rupture in the following way: A decohesion starts at the axis of the sample (the detailed features of which will be described by microfractography and discussed later); the flat cavity produced normal to the axis (on an average) grows radially by tearing apart at a moderate rate, and it then probably accelerates and suddenly forks into a conical shear fracture. Sometimes, instead of one single cone, two half cones of opposite directions are produced; a section of such a necked region in a radial plane containing the axis is shown in Fig. 3. This figure shows that the shear fracture starts at an angle of about 30° to the axis of the specimen and deviates progressively,

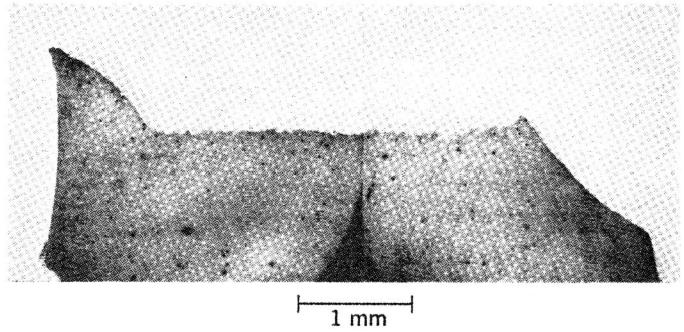

Fig. 3. Cross section of a tensile rupture showing two half cones

reaching the outer surface at an angle of about 45° or more. There is no sign of the outer portion of the neck moving as a wedge towards the center after the end of the first stage* (formation of the central fibrous zone).

An increase in hardness produces a decrease in the reduction of area at rupture. This is true whether the increase in hardness is due to an increase in testing temperature (up to 200°C) for the same steel or to a change in the heat-treatment of the steel tested at room temperature. In both cases, the slope of the curve (reduction of area versus ultimate tensile strength) is about the same.

For test pieces broken at higher temperatures or for harder steels tested at room temperature, the separation between the cup and the cone parts loses its sharpness, the bottom of the cup being rather wavy.

For metals such as copper or austenitic steel (35 Ni-10 Cr), Fig. 4 shows that between −200° and +200°C, the temperature has almost no influence on the appearance of the rupture surfaces and the reduction of area.

We shall not study here abnormal rupture appearances of the "milling cutter" type observed in hardened steels, which are due to low transverse properties.

* In some hard steels, where the rupture proceeds in a zigzag way along planes and not on conical surfaces, such wedge movements of parts of the metal, acting as a block, can be observed.

Comparison of Fatigue and Tensile Rupture Characteristics

If we now come back to the point raised at the beginning of the previous section, one has to take into account that, according to Bridgman, the true stress at the point of initiation of cup fracture on the axis is higher than the average stress.

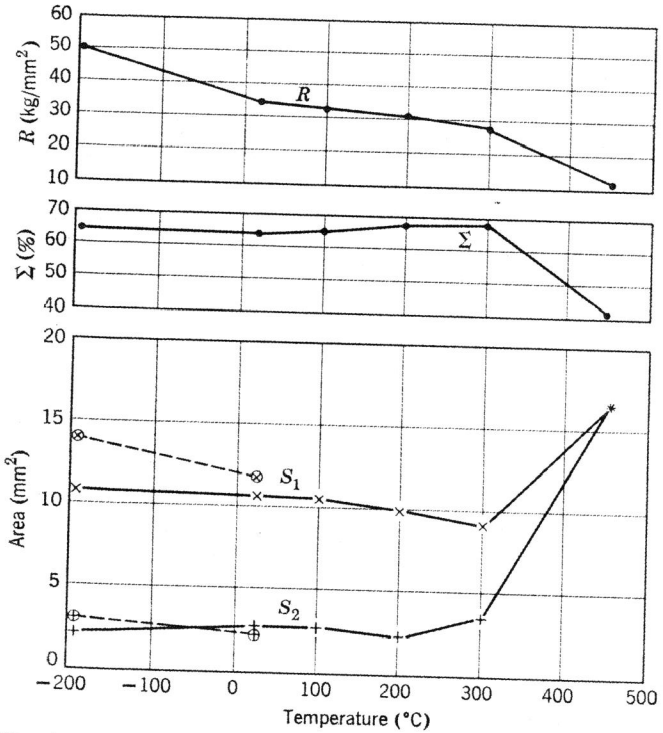

Fig. 4. Results of tensile tests on copper and (⊕⊗) austenitic steel (35% Ni and 10% Cr). R = ultimate tensile strength, Σ = reduction in area (%), S_1 = area of fracture surface, S_2 = area of bottom of the cups.

Although the Bridgman hydrostatic stress in the neck is difficult to evaluate precisely, one can roughly say that, for the tests on steel samples ground from fatigue-test pieces (reported in Fig. 1), the true breaking stress (at the center) is of the order of 135 kg/mm² for the softest sample and 180 kg/mm² for the hardest. The range of variation of the breaking stress is smaller than that of the fatigue limit, and the relation between these two quantities is far from being proportional. Moreover, the hardest steel has a lower breaking stress than the next harder one.

The conclusion is that the correlation between fatigue limit and true breaking stress (for initiation of cup-and-cone rupture) is far from being as good as that between fatigue limit and ultimate tensile strength (Fig. 1).

In the case of Al and Al-base alloys, the correlation between true breaking stress and fatigue limit is still worse; in refined Al (99.993%), the reduction of area reaches 100%, the rupture stress in the last section reaching 45 to 50 kg/mm²,[9] which is of the same order as the values observed for some light alloys.

On the other hand, it has been shown by fatigue tests conducted on notched samples at various temperatures between 20° and 600°C [7] that there is a good relation between the *notch sensitivity* found in these tests and the *percentage of cone area* in the cup-and-cone rupture of tensile tests conducted on the same steel at the same temperatures. This means that there is a parallelism between the factors influencing the two following phenomena:

1. Propagation* of a fatigue fissure from the root of a notch.
2. Propagation on an inclined surface of a combined shear and tearing process which starts from the tip of the growing central cavity, giving the cup part of the rupture in a tensile test.

Thin, Flat Specimens

A special mention should be made of the rupture surfaces of thin, flat specimens cut out of steel sheets or strips and tested in tension. After the maximum load, the necking and rupture occur in three stages:

1. General and tapered necking with reduction in thickness and in breadth.
2. A localized necking along a narrow band inclined to the tensile axis. The angle θ, made in the plane of the sheet by the direction of this necked band and the axis, has been measured on specimens cut in longitudinal, transverse, and 45° directions in very mild steel (OLP) strip. The results are reported in Table 2; they represent the mean value for

TABLE 2. Influence of Orientation on Ratio k and Angle θ

Sample Cut	k	θ (deg)
45°	0.87	63.6
Longitudinal	1.13	63.8
Transverse	1.40	62.9

* It is a question of propagation and not of initiation, since nonpropagating cracks can be observed at stresses smaller than the endurance limit.

about 160 tests, the scatter being smaller than 1° in each case. The same table gives the value of the ratio:

$$k = \frac{\text{contraction in breadth}}{\text{contraction in thickness}}$$

measured in the region of homogeneous deformation; this ratio is a measure of plastic anisotropy, applicable when the deformation is not too large.

If one hypothesizes that, in this band of necking, the elongation in the direction of the band is equal to zero (a condition that is necessary if zones of high distortion are to be avoided when the band is placed in contact with the surrounding undeformed portions of the sheet), one can calculate the value of k in the necked region:

$$k_n = \cot^2 \theta = \tfrac{1}{2}$$

The variations of k in the region of homogeneous deformation, as reported in Table 2, are small compared to the variation of k between that region and the neck. This is probably why the angle θ is rather insensitive to the orientation of the sample in the sheet.

3. In the necked band, a shear rupture occurs along a plane inclined to the plane of the sheet. In very pure soft metals (refined Al), this rupture is absent, the thickness of the necked band reducing progressively to zero.

Thus, in cylindrical specimens, one observes a one-stage necking and a two-stage rupture, while in thin, flat specimens, one observes a two-stage necking and a one-stage rupture, the stage corresponding to the flat cup part being absent.

Microfractographic Studies

Ductile Rupture Surfaces

Fibrous fractures. The microfractographs of fibrous ruptures always show the same appearance; the rupture surface has the appearance of a series of dimples on the two halves of the ruptured sample. Figures 5 and 6 give examples of this in a 30% Ni-Fe alloy and in an austenitic steel.

Very often, particles (inclusions or precipitates) are observed near the bottom of these dimples. This appearance helps us to understand the mechanism of this type of fracture. In the course of deformation and as a result of differences in elastic and plastic properties of particles and of the matrix, microcracks can be produced, either by cleavage of the

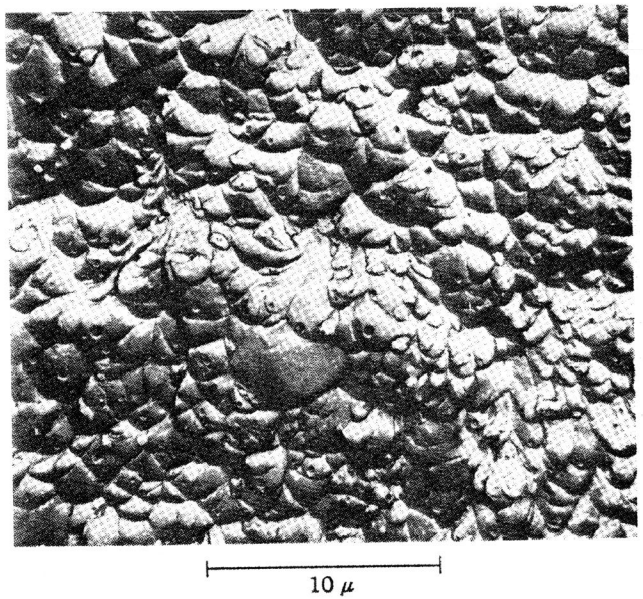

Fig. 5. Microfractograph of a fibrous rupture in a 30% Ni-Fe alloy containing oxide inclusions visible at the bottom of the dimples.

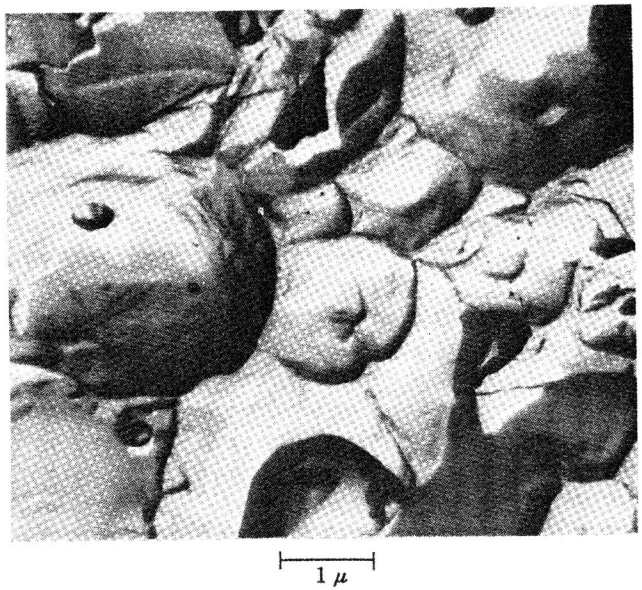

Fig. 6. Microfractograph of a fibrous rupture in an austenitic steel (18% Cr, 12% Ni).

particles or by decohesion between the metal and the particles. In front of the propagating rupture, in regions of high triaxial stresses, many such microcracks can form, or grow if they already exist, and produce the microholes observed as dimples in the microfractographs.

Figure 6 shows a typical case in which the shape of the dimples is influenced by the glide mechanism. Here the dimples are somewhat polyhedric. Moreover, at the bottom of the biggest dimple can be seen slip lines of different systems, which, on careful examination, are seen to be at angles of 60°. This suggests that the plane of the initial decohesion in the matrix must have been a slip plane.

The mechanism of the propagation of fibrous rupture, as deduced from microfractographic examination, is also confirmed by optical microscopic observations made on nickel-plated and polished transverse sections of ruptured or partially ruptured specimens. Figure 7 shows a section of such a fibrous rupture of mild steel in which, among others, a big dimple containing an inclusion is visible. Figure 8 is a section of the tip of the fissure in an impact-test specimen of mild steel which is incompletely fractured. Here holes that formed in advance of the propagation front can be clearly seen.

We have observed this fibrous type of rupture for carbon and alloy steels, austenitic steels, aluminum and light alloys, copper, brass, and even for such hexagonal metals as zinc and magnesium, although the dimples are less regularly shaped.

The role of second-phase particles is most important in the formation of dimples. It might be supposed that other obstacles to glide (grain boundaries, "relaxed" pile-ups of dislocations with intricate networks) could also initiate microcracks; but, as a matter of fact, in the very pure and clean metals we have studied, no fibrous fractures are to be observed. For example, refined Al (99.997%), pulled in tension, breaks with almost 100% reduction in area, the rupture surface reducing to a very small, rather smooth area of glide rupture; the same occurs for quenched Al-Cu alloy.

This role of particles explains why there should be a relation between inclusions and reduction of area, transverse properties and upper level of the impact strength (above the transition zone).

The distribution of inclusions or particles can influence the path of fissures: For instance, when these impurities are localized in the grain boundaries (intergranular precipitation), we can observe a kind of fibrous rupture, which follows the grain boundary. Numerous intergranular ruptures resulting from intergranular precipitation occur in this way.

Shear rupture. When the rupture surface is close to the plane of maximum shear stress, the appearance of the rupture is somewhat dif-

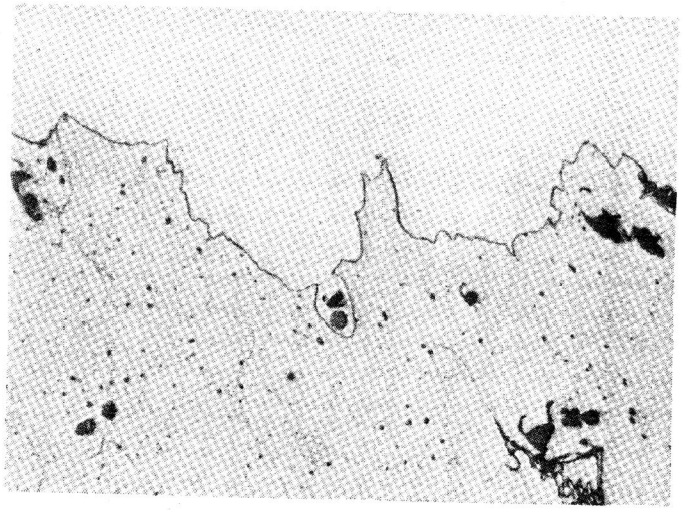

Fig. 7. Cross section of a fibrous rupture in mild steel showing an inclusion in the big dimple at the center.

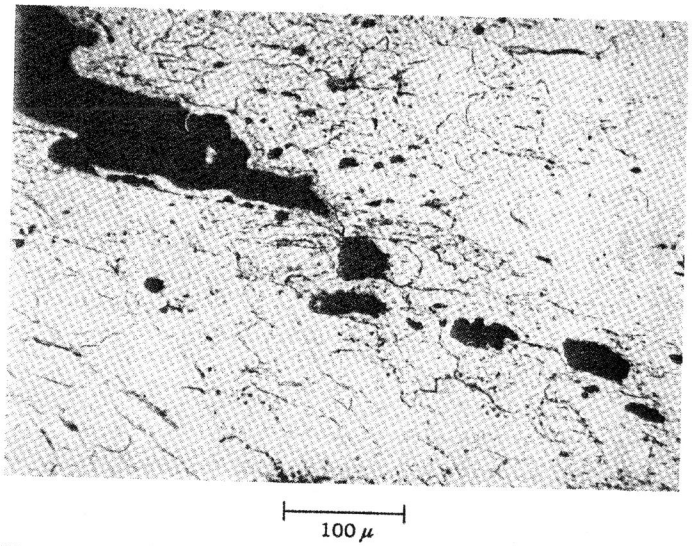

Fig. 8. Cross section of the tip of a fissure in an impact-test specimen of mild steel.

ferent. It includes some regions with elongated dimples, along with some rather flat decohesion regions.

Elongated dimples. Figure 9 shows a typical aspect of elongated dimples in which inclusions are also observed.

The dimples generally have the shape of a parabola or of a half ellipse. If the two opposite surfaces of a typical shear rupture are examined (a

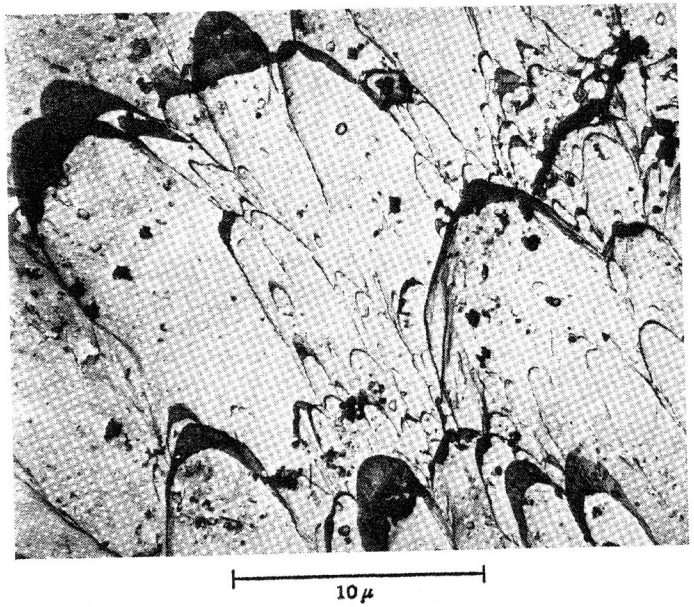

Fig. 9. Microfractograph of elongated dimples. Shear rupture surface of mild steel ruptured in bulge test.

cone surface of tensile rupture), it is observed that the concavity of these dimples is turned in opposite directions on the opposite faces, while the axis of symmetry is parallel to the direction of propagation of the rupture front. More precisely, for each surface viewed from above, the concavity is oriented towards the direction of relative displacement of the other half of the specimen.

These appearances would be expected if, in a layer (HH' in Fig. 10) suffering a heavy local shear (indicated by arrows in the figure), an inclusion starts a microcrack, as in the case of fibrous rupture. This microfissure, first normal to the direction of maximum tensile stress, is progressively distorted by local shear, as shown in Figs. 10*b* and *c*. If the shear concentrates in a thinning layer (a mechanism that is enhanced by the growth of the microfissures and the corresponding increase of

stress on the remaining metal portion), rupture finally occurs along a plane (AB in Fig. 10c).

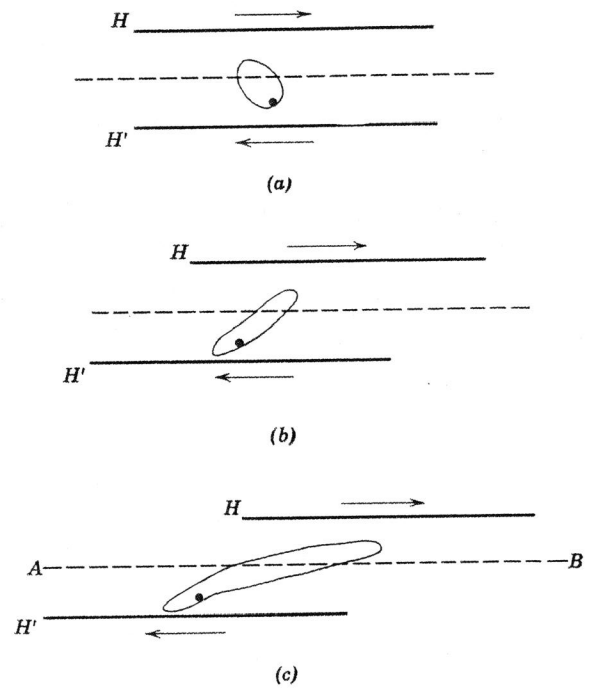

Fig. 10. Schematic representation of the formation of an elongated dimple. (*a*), (*b*), and (*c*) represent successive stages.

Decohesion along glide planes. The shear rupture surfaces often show, besides regions covered with elongated dimples, rather flat areas, more or less extended, as can be seen in Fig. 11.

The same type of decohesion has also been observed on normal tensile or impact-test rupture surfaces of mild steel in the fracture-transition temperature zone. It is observed more frequently in areas where brittle cleavage fracture stops and is replaced by ductile fracture. Figure 12 shows the section of a corresponding rupture surface, where several transcrystalline facets make a significant angle (about 45°) with the mean direction of the rupture surface. As the microfractographic aspect of these facets is quite different from the brittle cleavages, another fracture mechanism must be inferred. *It may be that fracture occurs in slip planes that have been weakened by deformation.* This assumption is sustained by the following observations.

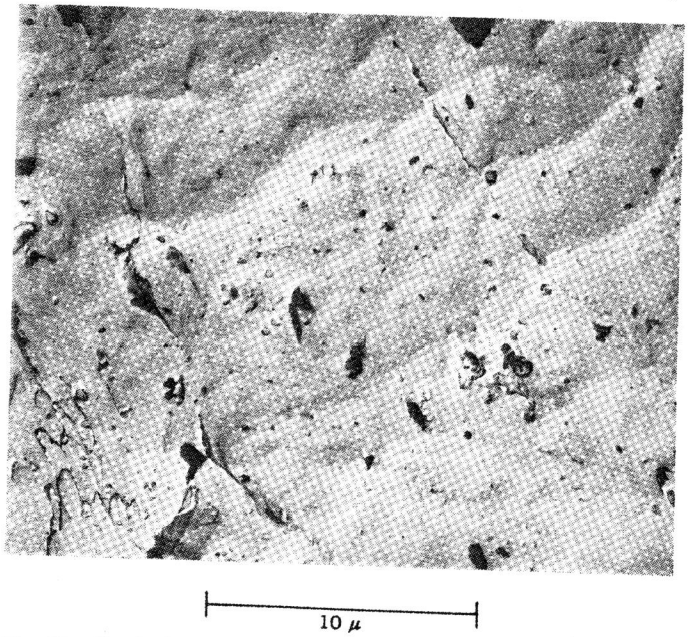

Fig. 11. Typical microfractograph of "decohesion along glide plane." Same rupture surface as for Fig. 9.

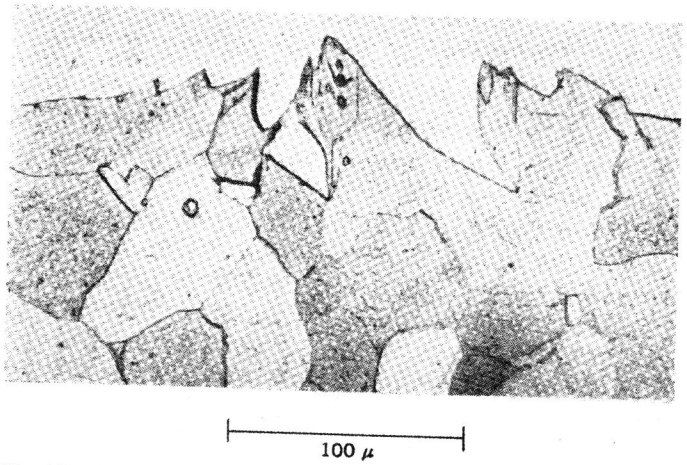

Fig. 12. Cross section of the rupture surface of an impact-test specimen broken in the fracture transition range. Pearlite-free steel, tested at −30°C.

1. It has been shown earlier [3] that, for prestrained specimens broken in the fracture-transition range, flat facets of decohesion along oblique planes are very frequent. These oblique planes are presumed to be glide planes that were active during the prestrain.

2. There is a change in the orientation when the rupture changes from a normal cleavage to a decohesion of the type studied here. Thus, although the average orientation of the rupture surface is in this case normal to the tensile stress, these facets must be produced by a local shear.

3. It is not possible to make any distinction between a big dimple of a fibrous rupture, if it is rather flat, and the type of decohesion already described, an observation in agreement with the afore-mentioned statement that initial decohesions producing dimples may be along glide planes.

On zones of decohesion along glide planes, somewhat isolated dimples, which are always extremely elongated, can be observed (Fig. 13). It

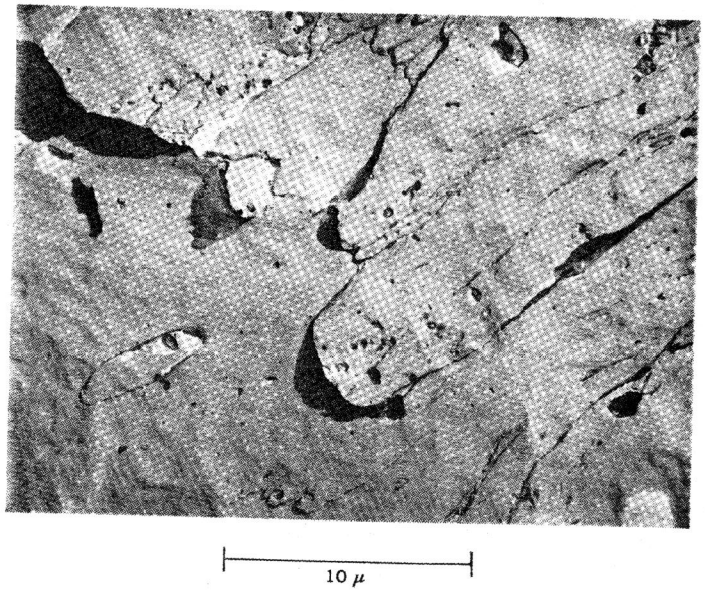

Fig. 13. Microfractograph of a "decohesion along glide plane" with very elongated dimples. Same rupture surface as in Fig. 9.

seems difficult to assume that such a large amount of elongation is produced by a mechanism of local shear, as described earlier (Fig. 10). It is more probable that, in this case, the microcracks responsible for the formation of the dimples are initiated only a small distance in front of the propagating fissure and in such a way that the front merges rapidly with the growing microcrack, thus giving rise to parallel lines of tearing.

Occurrence of Fibrous and Shear Ruptures

Having thus described the main features observed in the various surfaces of ductile rupture, we shall now see in which type of testing they occur.

In tensile tests on cylindrical specimens, under conditions excluding low-temperature brittleness and high-temperature intergranular brittleness, the ruptures are generally of cup-and-cone type, as mentioned earlier. Microfractographic examinations show that the cup area has a fibrous appearance, with no decohesion along glide planes. On the other hand, the cone area shows the typical appearance of a shear fracture, in which elongated dimples are mixed with decohesion zones along glide planes, the proportion of the latter zones being about 20% for a test piece broken at room temperature.

In a similar manner, for impact-test pieces broken at temperatures higher than the transition range, the portion of the rupture surface that is nearly perpendicular to the axis of the specimen is of the fibrous type, while the shear lips are composed of elongated dimples and zones of decohesion along glide planes.

For lower test temperatures, the central portion of the rupture surface may be brittle and extension of the shear lips reduced, but otherwise their appearance is unchanged.

Thus it seems that two very different types of rupture, either fibrous or brittle, may turn to shear rupture when the general direction of the fissure is changed. It seems important to point out that the speed of propagation for shear rupture is in a range intermediate between the speed of propagation in cleavage and fibrous rupture. Therefore, the occurrence of the shear rupture corresponds, at higher temperatures, to an increasing speed of propagation, while it corresponds, when the main fissure propagates in a brittle manner, to a lowering of the propagation speed.

The detailed observation of a rupture with *mixed* features also leads to the conclusion that the transition from cleavage to fibrous rupture is not usually abrupt; on the contrary, its occurrence is usually accompanied by the formation, immediately following the cleavage, of more-or-less extended areas of glide decohesion, then by elongated dimples, and then by equiaxed dimples. These successive forms correspond to a progressive lowering of the propagation speed.

Turning now to samples cut from sheets, we have observed, both in tensile and in deep-drawing tests, that the rupture which occurs after the reduction of area along a band is of the shear type. However, the ratio of glide decohesion areas to dimpled ones is about 50% in tensile tests and 20 to 30% in bulge or Erickssen tests, a difference that may be related to the biaxial stresses of the latter type of test.

Finally, the fracture surfaces of specimens cut from the same sheet and broken in a repeated bending test (after 18 cycles) have shown that, of the total area, of the order of 70% was glide decohesion area, which presents essentially the same appearance here as it does in the steady unidirectional type of test (tensile test). This leads us to make a more general comparison between the aspects of rupture observed in unidirectional and in oscillating stress tests.

Fatigue Rupture

Appearance of fatigue rupture surfaces. In the case of fatigue ruptures,[10] the decohesion is known to occur along deconsolidated slip planes, and one may expect to observe regions of glide decohesion analogous to those described earlier. However, as observed from the deformation bands on the surface of fatigue specimens, the deformation that provokes the deconsolidation differs here from the deformation in the samples where rupture occurs by a unidirectional deformation, such as in a tensile test. The propagation of the rupture along the glide planes in the two cases also appears to be very different, and this difference is clearly visible on microfractographs: In the case of fatigue, very smooth areas are rather rare, the rupture surface often being covered by more or less regular striations of the type shown in Figs. 14, 15, and 16. These figures pertain to mild steel, duralumin, and 18-8 stainless steel, respectively. Figure 17 shows a zone containing straight striations regularly spaced at about $\frac{1}{4}\,\mu$, a feature sometimes observed in fatigue rupture of stainless steel.

The principal observations of fatigue rupture surfaces reported here concern mild steel specimens and pertain chiefly to striations as regards their orientation, spacing, and relation to the rupture propagation front.

Relation between striations and the propagation front of fissures. By carefully identifying the replica orientation, we have been able to specify that the striations are, in general, perpendicular to the direction of the propagation front. This result, which may indicate that striations represent successive positions of the propagation front, has also been verified by optical microscopy in those cases in which the spacing of striations was sufficient to be resolved at low magnifications. After comparison of the striations on specimens ruptured in a variety of tests during which the speed of propagation of the fissures was measured, it can be concluded that the striations will be spaced farther apart the higher the velocity of propagation of the fissure. Optical microscopic observations have also been made on the rupture surface of a rotating-bending specimen. The speed of propagation of the fissure increases as it progresses, and optical microscopic observations on successive zones of the surface of rupture have confirmed that the orientation of striations is perpendicular to their direction and that their spacing increases progressively.

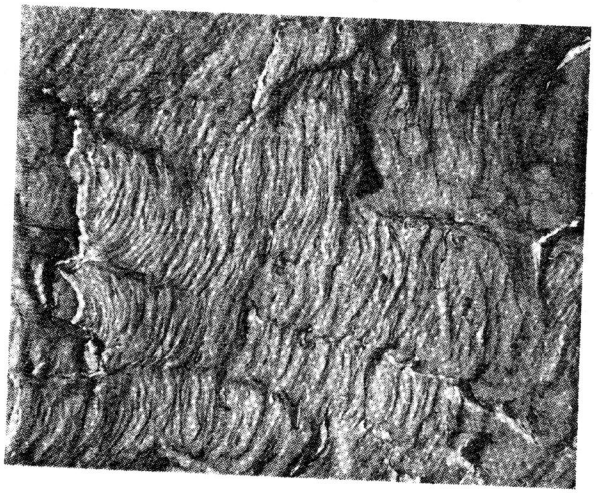

Fig. 14. Microfractograph of a fatigue rupture surface of mild steel (rupture in 0.64×10^6 cycles under 12 ± 19 kg/mm² direct stress).

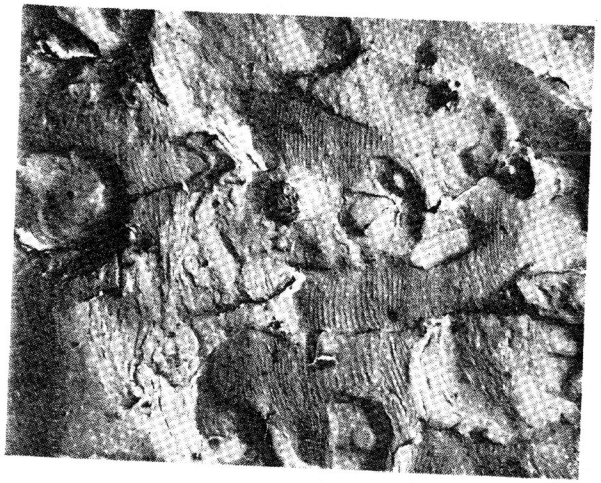

Fig. 15. Microfractograph of a fatigue rupture surface of duralumin (alternate bending, ± 7 kg/mm², rupture in 0.27×10^6 cycles).

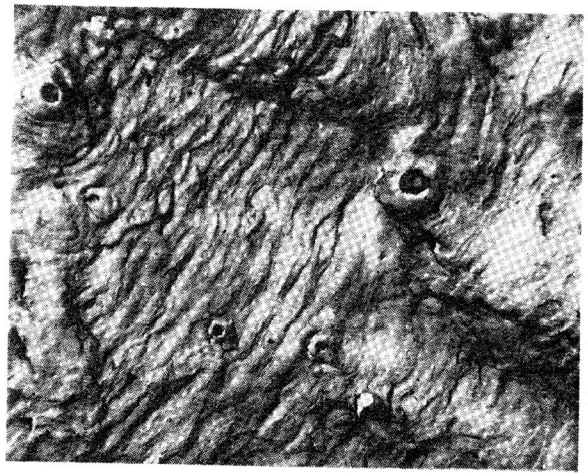

Fig. 16. Microfractograph of a fatigue rupture surface of 18-8 stainless steel (direct stress, ± 23 kg/mm², rupture in 77,000 cycles).

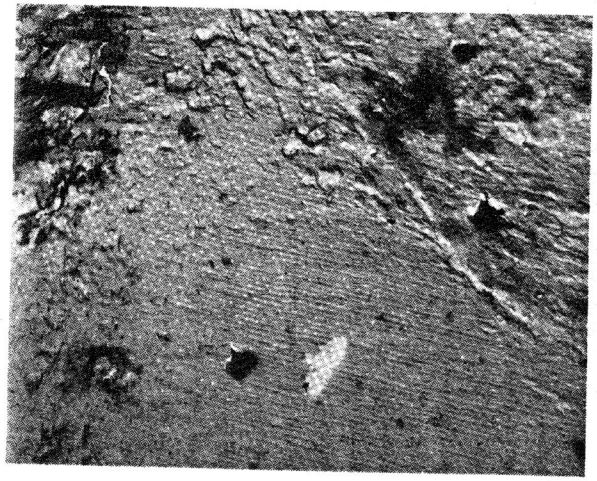

Fig. 17. Microfractograph of a fatigue rupture surface of 18-8 stainless steel (rotating bending, ± 24 kg/mm², rupture in 0.87×10^6 cycles).

In order to specify the number of stress cycles that corresponds to the successive striations that indicate the passage of a rupture front, we have tested some Charpy U-notched mild-steel specimens by repeated bending on constant-moment type machines. Because the propagation front of the fissure in such a test is essentially straight and perpendicular to the lateral faces of the specimen, the depth of the fissure can be measured easily by the apparent length of fissure on its two side faces. The microfractographic technique was utilized to measure the spacing between the successive striations. These measurements, although not precise, indicate definitely that the passage of the rupture front from one of the striae to the next requires one cycle or, at the most, a few cycles of stress.

Often the striations present a curved front (festoon type) convex to the direction of propagation. The extremities of successive festoons are more or less aligned in a direction perpendicular to the rupture front and to the average direction of striations (Fig. 14). The resulting markings on the surface of the rupture represent ridges formed by tearing. The local deformation, which results in this tearing, retards propagation of the fissure. This explains the occurrence of these festoons.

Relation between the striations, grain boundaries, and tear lines. In the microfractographs of fatigue-ruptured surfaces, the grain boundaries are neither visible nor indicated by discontinuities in the striations. In order to locate the position of a grain boundary in the microfractographs, it is necessary to etch a fatigue-ruptured specimen, but very lightly so as not to dissolve the striations. Figure 18 shows microfractographs of rupture zones containing grain boundaries and striations. The grain boundaries are in no way seen to affect the striations.

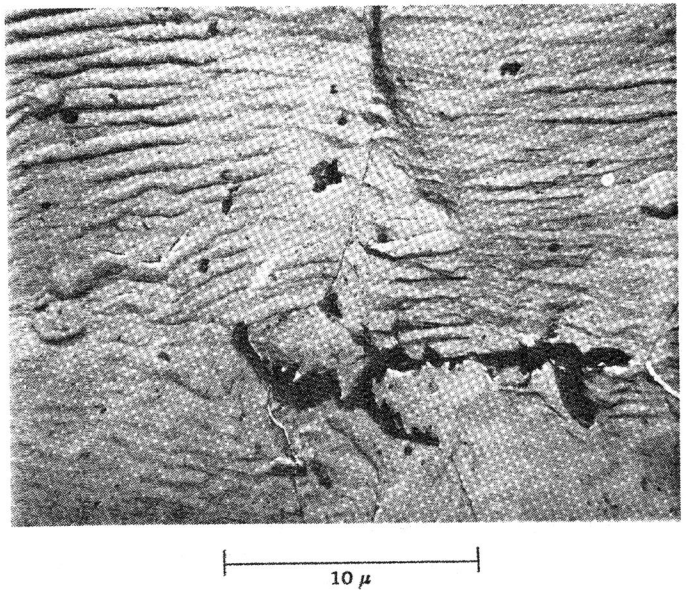

Fig. 18. Microfractograph of a fatigue rupture surface of mild steel after slight etch showing grain boundaries (direct stress, ± 25 kg/mm², rupture in 0.29 × 10^6 cycles).

Role of inclusions or precipitates in the propagation of fatigue ruptures. The appearance of striations in the vicinity of inclusions and precipitates (Figs. 15 and 16) may give some indication of the role played by particles in the propagation of fatigue ruptures. In Fig. 15, it can be seen that the plane of rupture deviates in the vicinity of the inclusions, while, in Fig. 16, the shape of the striation around the particles is an indication that small zones of decohesion form at the inclusions in front of the propagating rupture and that they later join the main fissure.

Influence of previous cold-work on fatigue ruptures. Mild-steel specimens prestrained to 5, 10, and 15% in tension were ruptured in fatigue (unsymmetrical tension-compression). The microscopic examination of rupture surfaces showed different appearances:

1. The rupture after zero prestrain, at least that in the zone with a slow speed of propagation of rupture, was more or less plane and normal to the stress axis.

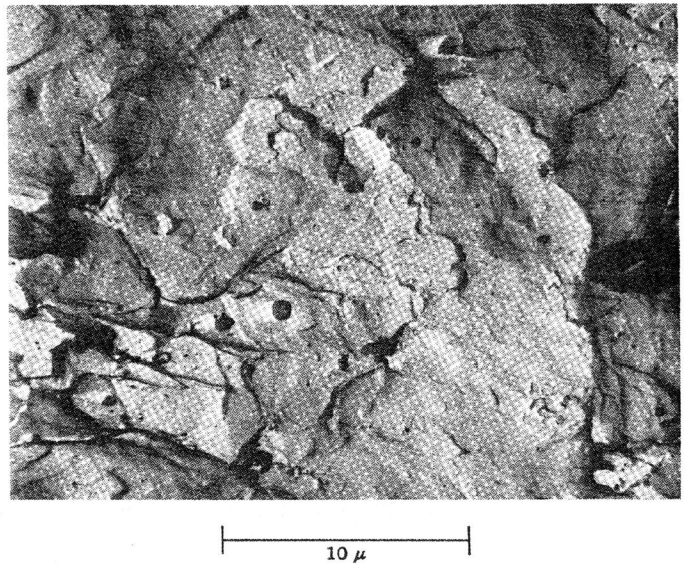

Fig. 19. Microfractograph of a fatigue rupture surface of mild steel after 15% prestrain in tension (rupture in 0.62 × 10^6 cycles, direct stress 10 ± 16 kg/mm²).

2. After 5 to 10% prestrain, the rupture surface was plane, but it made an angle of about 45° to 60° with the stress axis.

3. After 15% prestrain, the rupture surface had a marked relief without a clear-cut general orientation.

Observations by microfractography show a continuous evolution as the prestrain increases. After 5% prestrain, the striations on the rupture surface are less regular, more sinuous, and shorter, as compared to ruptures with 0% previous cold-work. The irregularity of striations in the case of ruptures occurring after 10% prestrain is more accentuated; all surfaces of decohesion along glide planes show ill-defined striations. This change is also true of 15% prestrained samples, where striations can no longer be identified, but here there appear disturbed and rounded zones, similar to dimples (Fig. 19), which contain inclusions.

Features similar to those described for prestrained specimens are observed in fatigue ruptures when the specimen suffers a macroscopic deformation during fatigue because of the mode of its application (for example, unsymmetrical tension-compression).

Microscopic Observations of Slip Bands

For a better understanding of the differences in the appearance of rupture surfaces, we have examined at both optical and electron magnifications the appearance of the bands that develop superficially in unidirectional or repeated stress tests.

Tensile Deformation

Figures 20 and 21 show the slip bands on the surface of a cylindrical tensile specimen deformed to rupture at 20°C. The optical view shows many sinuous slip bands; this sinuosity is a consequence of easy cross slipping. In most grains, there is a simple predominant direction for these bands. In the electron micrograph, the slip bands are seen with low contrast owing to their diffuseness.

Some observations made on test pieces deformed at 160°C show, as a general trend, more numerous, better-defined slip systems in each grain (Figs. 22 and 23). On electron micrographs, these slip bands appear sharper, resulting from a more localized deformation.

Repeated Stress Tests

In fatigue testing, the surface bands (Figs. 24 and 25) are broader than they are in the preceding cases. The electron microscope shows slip lines within these surface bands, the direction of which is not always parallel to the bands. Some of these slip lines appear very dark, and, as suggested by Hempel,[11] they may correspond to microcracks. It may

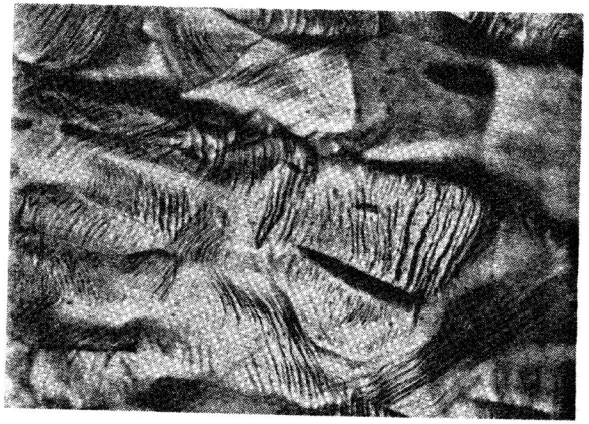

Fig. 20. Optical micrograph of the cylindrical part of the surface of a mild-steel sample deformed to rupture showing slip bands.

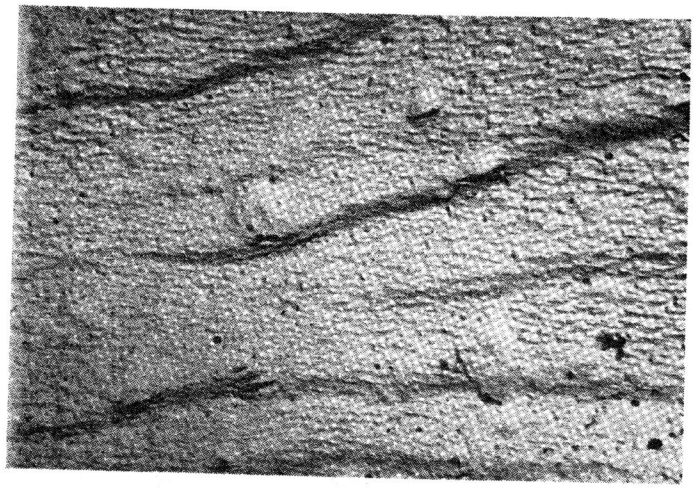

Fig. 21. Electron micrograph of the same surface shown in Fig. 20. The engraved appearance of the surface is due to electropolishing.

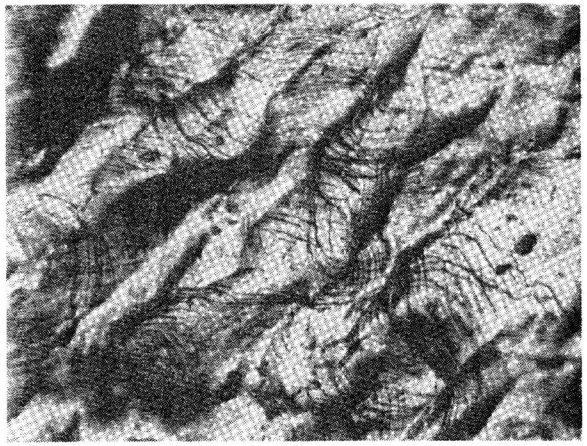

Fig. 22. Same surface as in Fig. 20 but after a tensile test conducted at 160°C.

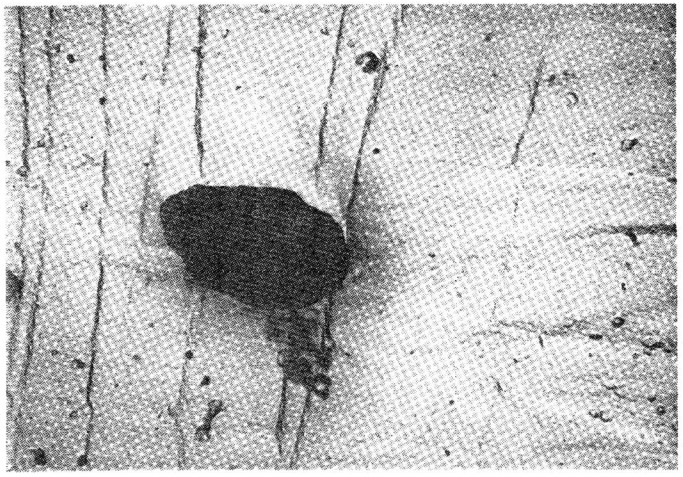

Fig. 23. Electron micrograph of the same surface as shown in Fig. 22.

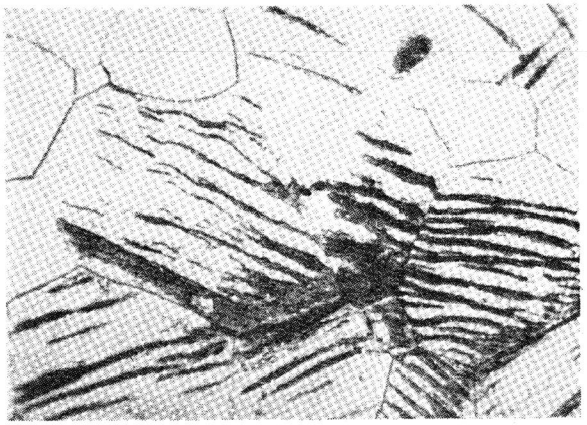

Fig. 24. Optical micrograph of the surface of a flat specimen fatigued in alternate bending (525 cycles at ± 13 kg/mm², not ruptured).

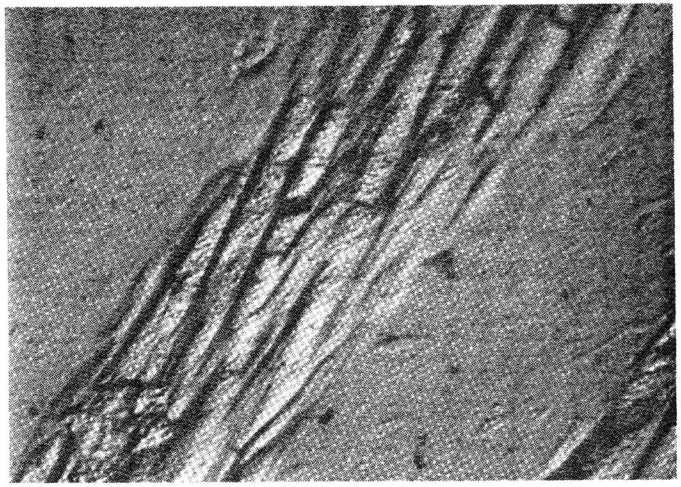

Fig. 25. Electron micrograph of a sample identical to that of Fig. 24.

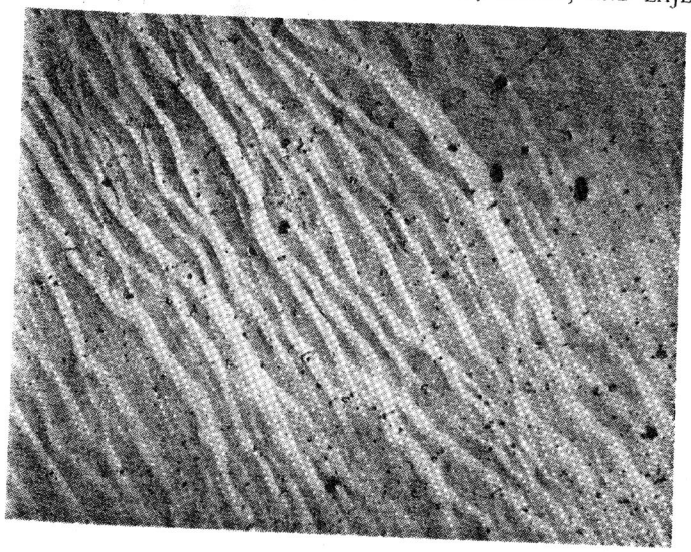

Fig. 26. Electron micrograph of the surface of a mild-steel sheet after 1 bending cycle, repolishing, and bending again.

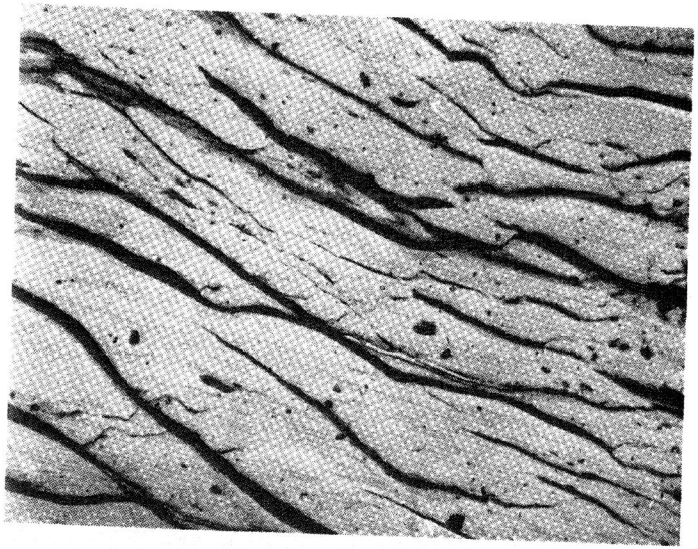

Fig. 27. Electron micrograph of the same specimen as shown in Fig. 26 after 14 bending cycles, repolishing, and bending again.

be noted from Fig. 24 that the fatigue bands may go through grain boundaries without much deviation, a situation analogous to that observed for striations on rupture surfaces.

For high-stress repeated bending at a low number of cycles and with a large amount of plastic deformation, the features observed are somewhere between those observed on tensile and fatigue specimens.

In order to follow the evolution of deformation bands, we have carried out the following tests:

1. An electropolished sheet of mild steel was bent at 180° on a cylindrical head 4 mm in diam, and a micrograph taken (Fig. 21).

2. The sheet was then restraightened and repolished. After a new bending at 180°, the micrograph in Fig. 26 was taken.

3. The same test was repeated after 14 bending cycles (Fig. 27). The number of cycles to rupture was 18. The figure shows very marked slip bands, but they are narrower than those observed in fatigue; their appearance suggests extruded zones or microcracks.

A comparison of these three successive views gives the following information:

1. Unidirectional deformation gives a diffuse, rather unlocalized deformation with wavy slip bands (diffuse cross slipping).

2. Successive cycles intensify the localization of deformation along better-defined glide planes (or fragments of planes). This localization may result in superficial extrusion, intrusion, or microcracks, even after a very small number of cycles. One must remember that, with the repolishing technique used, only the new deformation at each cycle is observed, and this can be localized on the outer zone of a fatigue band (between a fatigue band and previously undeformed metal).

Discussion of Results

The observations reported in this chapter deal generally with the propagation of rupture. One must bear in mind that even critical stress conditions represent conditions at which the propagation of a rupture is possible after the initial microcrack has attained a critical size. It is only for subcritical sizes that the formation of a microcrack involves factors or phenomena that are specifically related to the initiation state.

Thus the following discussion will treat problems related to rupture propagation. Nevertheless, in the course of such a propagation, reinitiation of small subsidiary cracks does very frequently occur in front of the tip of the growing fissure; discussion on that point will give useful information on the phenomena occurring during the initiation stage.

The main subject of this chapter is a comparison of ductile and fatigue

rupture. The experimental results presented in the preceding sections show many similarities between these two modes of fracture:

1. There is a good correlation between fatigue endurance limit and ultimate tensile strength of ductile metals.

2. Significant portions of the fatigue rupture surfaces are composed of facets of decohesion along glide planes, which are also frequently encountered in ductile fracture in places where fracture occurs by a shear mechanism.

3. The appearance of the fatigue rupture surfaces of prestrained specimens or of specimens undergoing an over-all deformation during test is similar to surfaces of shear rupture.

4. Rupture surfaces of specimens fatigued at high strains and broken in a small number of cycles (repeated bending) have the same appearance as the rupture surfaces of ductile shear fractures; only the relative proportions of areas occupied by dimples or by decohesions along glide planes are different.

5. The fatigue bands produced in the repeated bending specimens mentioned in the preceding paragraph, despite the small number of cycles, have some of the characteristic features (intrusions and surface microcracks) observed in samples fatigued for a great number of cycles.

6. The density of inclusions on both fatigue and shear rupture surfaces for the same steels is of the same order. In both cases, the fracture can deviate slightly from its mean path in order to pass by an inclusion. This deviation occurs in such a way that a microcrack formed around the inclusion before the passage of the rupture front merges with the rupture front. The only difference between the two types of rupture is that this microcrack is smaller and more round in fatigue, while in shear rupture it is elongated by the high local shear (elongated dimples).

7. In tests conducted above room temperature, the notch sensitivity in fatigue is related to a characteristic of the tensile rupture, namely, the area of cone shear rupture.

Despite these similarities in the two types of rupture, there are a few big differences, the most important being:

1. In the regions not covered by facets of decohesion along glide planes, the appearances are quite different: The ductile fracture is characterized by dimples (equiaxed or elongated) and the fatigue fracture by striations.

2. The endurance limit, which is the critical stress for fatigue rupture, cannot be easily correlated with the critical stress for tensile rupture (the true breaking stress in cup-and-cone fracture). It must be remarked that in the latter case the initiation of rupture occurs in a zone of fibrous fracture where no decohesion along glide planes is to be found, which

means that no similarity in the appearance of rupture surfaces exists at that place.

3. The endurance limit can be correlated with the ultimate tensile strength, but this is not a critical stress for decohesion but a representation of the results of a balance between strain hardening and "geometrical softening."

4. In the two fracture surfaces showing similarities (fatigue and shear fracture), the rate of propagation of the fissure is very different, being very slow for fatigue and very rapid for shear fracture.

In order to reach a better understanding of these similarities and differences, we must now analyze in more detail some factors of each of these two rupture modes.

Ductile Rupture

In ductile ruptures, inclusions play an important role. This can be illustrated by a comparison of microfractographs of the same steel broken in a brittle or in a "tough" condition: [3] On cleavage facets, almost no inclusions can be observed; one can say that cleavage ignores or even avoids inclusions, while a ductile rupture has a tendency to incline its path by way of inclusions. This is particularly marked in fibrous rupture, where one can say that the rupture directs its path through inclusions, jumping from one to the other. This is true for the zones of elongated dimples of shear fracture, but not for decohesion along glide planes, where the density of inclusions is small and normal.

The difference between the various forms of fibrous or shear rupture is mainly due to two factors: rate of propagation and nature of the stress field. The influence of the rate of propagation can be analyzed in the following way. If the propagation is slow, the tip of the fissure has time to round off by plastic deformation; the zone of stress concentration in front of the tip is rather broad and thick (Fig. 8), causing many inclusions, around which microcracks are formed either by cleavage of the particles or by decohesion between the metal and the particles.* These microcracks also have time to round off before being joined by the fissure front; thus the fracture path jumps from hole to hole. An important factor in this "rounding off" of microcracks is the very high triaxial stress system: This facilitates glide on multiple systems, as well as all accommodating processes like climb or cross slip.

* The piling-up of dislocations around inclusions and the very intricate dislocation networks formed on "relaxed pile-ups" play an important role in the initiation of these microcracks by producing flat, annular zones of low cohesion where a local "decohesion along glide planes" can start, as proved by some observations.

When the crack accelerates, the tip of the notch becomes sharper, and the stresses at the tip become higher and concentrate in a narrower zone. If other embrittling conditions are present (such as low temperature), this may turn into a brittle fracture, a case that has been studied elsewhere.[3] However, if the triaxiality is low and brittle fracture impossible, as in the narrow peripheral zone around a central cup fracture or in the lips of an impact-test specimen, the accelerating fissure can turn into a shear fracture. A careful study of electron microfractographs shows that the transition between fibrous and shear zones of fracture is not sharp: The dimples become progressively elongated while the percentage of glide decohesion facets increases.

The reason for the deviation of the rupture path from fibrous decohesion, normal to the tensile stress, to oblique shear fracture is not entirely clear. It includes the following factors:

1. There is a decrease in the triaxiality of the over-all stress field (not including the stress concentration at the tip of the fissure), which favors the glide processes.

2. There is an increase in rate of propagation of the fissure front, which produces, as stated previously, a narrower fissure and a smaller radius at the tip; hence, the distribution of stress tends to be analogous to that described by Kies, Smith, and Irwin:[12] When a microcrack initiated in front of the tip reaches regions at a small distance from the mean plane of the fissure, it finds there high shear stresses that hinder the rounding off of the hole and encourage glide decohesion processes.

Once a shear process starts, it tends to localize in narrow layers because of local heating, as required by Zener's "adiabatic shear" theory, and the production of microcracks and microholes in front of the fissure. The latter reduces the actual cross-section area along the plane of shearing and thus increases the actual shear stress.

As stated above, under these rapid propagation rates of fissure, the zone of stress concentration that is capable of initiating a microcrack around an inclusion is very narrow, and thus, only a few inclusions can play an important role in this process. This fact explains why the density of inclusions and elongated dimples becomes smaller with faster rates of propagation.

As a limit, at very fast rates, no more dimples are produced, and the rupture surface presents the appearance of "decohesion along glide plane." This must be produced by a very acute fissure, pushing in front of its tip and along its plane a cluster of dislocations that helps decohesion. In this case, if an inclusion lies near the (future) plane of shear decohesion and if the propagation is not too fast for a microcrack to be initiated, a dimple starts forming a small distance in front of the propagating rupture; the latter soon joins the dimple and merges with it producing only two lines of tear.

Such decohesions along glide planes are actually observed in two cases:

1. When shear rupture is generated from an accelerating fibrous rupture, as described above; in this case, the over-all deformation preceding rupture is high.

2. When shear rupture stops a decelerating brittle fracture. In this case, the over-all deformation preceding rupture is not very high; for mild steel, it may be of the order of 30%.[3]

Fatigue Rupture

When studying the fatigue rupture mechanism, one must bear in mind that the phenomena are not the same at the surface and in the inner volume of the specimen. Thus, although many recent studies have emphasized the role of surface extrusions, intrusions or microcracks (and these surely do play an important role in the superficial initiation of fatigue rupture), their presence at the surface does not mean that microcracks are to be found inside the metal (since extrusions are not possible in the interior). It is reasonable to assume that, except for the zones surrounding inclusions where "decohesion along glide planes" may produce annular microcracks, no *actual* microfissures exist inside the metal.

Thus, the fissuring must occur just in front of the tip of a propagating fissure. This is confirmed by the relation observed between the spacing of striations and the rate of propagation of the fatigue crack front.

It may be noted that observation of a fatigue crack growth on the surface of a sheet subjected to alternate bending shows that the crack does not prefer zones with high density of fatigue bands for its propagation. This seems to confirm the conclusion that the local strain just in front of the tip is more important in the propagation mechanism than the strain suffered by the same region during the previous fatigue life.

Regarding the origin of striations on the fatigue rupture surfaces, an important fact is that they generally are of noncrystallographic orientation, since they are not usually influenced by grain boundaries. Under unusual circumstances, they may be straight and take crystalline orientations (Fig. 17); this is probably the case when they are parallel to a Burgers vector. Thus, dislocations parallel to the fissure front will be of the screw type and will be capable of easily changing their glide plane by cross slipping. This suggests that, in front of the fissure tip, dislocations are put in a to-and-fro motion in a small zone of a glide plane; this movement, which will not be discussed in detail, probably results from accumulation of vacancies, multiplication of jogs, or nonconservative movements. It will produce a loss of cohesion. If jog formation is diffi-

cult in the metal considered and if the orientation is favorable, straight steps will be formed as shown in Fig. 17; but, in this general case, when many jogs or cross slippings can occur, the steps will be wavy and irregular. This is especially marked in ferritic steel, where cross slipping is easy, as can be seen from the appearance of broad fatigue bands on the surface.

Even in austenites, the presence of wavy striations proves that, at least locally in front of the fissure tip, a state of deformation is reached where the density of dislocations is such that many jogs (or vacancies) are produced. In other words, the local strain corresponds to the portion of strain-hardening curves for single crystals generally called "part III," the part beyond the "transition point" of a stress-strain curve.[13,14] This confirms Mott's theory of fatigue.

This mechanism can be repeated in successive planes, a fact that explains why the striations have a mean orientation parallel to the propagation front.

Comparison of Fatigue and Ductile Ruptures

There is no apparent relation between the mechanism of fibrous and fatigue rupture. This is why no good correlation is found between fatigue endurance limit and either the true breaking stress in tensile tests or resistance to torsion.

On the other hand, great similarities exist between fatigue and ductile shear rupture, as have been emphasized. It must be noted that the shear rupture of a cone-type tensile rupture is a consequence of fibrous rupture. The minimum strain at which shear rupture can occur must be sought in that type of shear rupture occurring between brittle fracture and the shear fracture with dimpled surfaces. We have seen that this occurs at a strain of the order of 30% (for mild steel), which is a little beyond the transition point of tensile curves. A local strain of the same order is required for fatigue rupture.

This similarity explains why the fatigue limit should be related to the stress reached in "zone III" of the tensile curve, where the strain is of an order not far from the maximum load or ultimate tensile strength.

In both cases (fatigue and shear), the decohesion must start along a facet of "decohesion along glide plane." Other such facets may be found later in the propagation zones. In both cases, the fissure is very narrow, with the consequence that the density of inclusion encountered is rather small.

Of course, great differences exist between the propagation mechanism of shear rupture and that of fatigue: Particularly noticeable is the presence of elongated dimples in the former and striations in the latter. This is due to the large difference in propagation rate and distribution of strain. Prestraining a fatigue specimen changes the strain distribution in such a way as to make it more uniform, and it also gives to the surface a fatigue-rupture appearance that is more similar to that of shear rupture.

Summary and Conclusion

1. Tensile and fatigue tests have been performed at room temperature on a number of ferritic steels treated to various hardnesses. Mild and medium carbon steel have been tested in the same way at various temperatures (20° to 600°C). Some tests have also been conducted on other metals (stainless steel and copper). In each case, the number of samples tested was large enough to give a good statistical basis. Some torsion tests and hardness measurements have also been made.

2. The fatigue limits deduced from these tests have been compared to various mechanical properties deduced from the static tests (ultimate tensile strength, true breaking stress, yield stress, resistance to torsion, and hardness). The best correlation is found between ultimate tensile strength and fatigue limit.

3. The macroscopic appearances of tensile ruptures have been observed on cylindrical or thin, flat samples. The necking and rupture mechanisms have been compared in both cases.

4. A microfractographic study has been made of these various types of rupture.

5. At large magnification, two features are observed on ductile rupture surfaces:

   (*a*) Equiaxed dimples are seen on fibrous fractures. The density of inclusions is very high in this case; an inclusion is almost always found at the bottom of each dimple.

   (*b*) Shear fracture surfaces are composed of elongated dimples and facets of "decohesion along glide planes." In this case, the density of inclusions is not so high.

6. Fibrous ruptures are found at the bottom (cup) of the tensile rupture of a cylindrical specimen or on the central part of impact-test specimens broken above the transition range. Shear fracture can occur on the peripheral zone (cone) of tensile ruptures, on shear lips of impact-test specimens, or it can cover the whole thin-sheet rupture surface.

7. From the point of view of propagation rate, shear fractures are produced either by an accelerating fibrous rupture or by a decelerating brittle fracture.

Detailed observations of the appearance of these ruptures show that the facets of decohesion along glide plane are associated with a higher rate of propagation than the elongated dimples.

8. The microfractographic study of fatigue rupture surfaces shows some facets of glide decohesion, which are rarely very smooth; most of the surface is composed of striated areas.

9. Inclusions may turn the fissure towards them. They appear surrounded by small annular zones of microcracks probably formed in front of the tip of the growing fissure.

10. The density of inclusions is about the same on fatigue and shear rupture surfaces, showing that in both cases the fissure is very narrow, the zone of stress concentration at its tip sweeping only a thin layer.

11. Some surface micrographs have been taken of slip bands produced either by tensile tests of cylindrical specimens at temperatures up to 180°C, by repeated bending (it is noted that 14 cycles of high strain are sufficient to produce intrusions or microcracks characteristic of fatigue solicitation), or by fatigue tests with a high number of cycles.

12. The mechanisms of propagation of ductile and fatigue ruptures have been discussed in detail.

13. A similarity exists between shear and fatigue ruptures, both occurring partially by "decohesion along glide planes." This is due to a sharp localization of the deformation either preceding (fatigue) or accompanying (shear) the propagation of rupture. The strain reached for this propagation is of the same order in both cases; only the distribution is different. This confirms Mott's theory of fatigue and explains the correlation between fatigue limit and ultimate tensile strength.

REFERENCES

1. R. Cazaud, *Fatigue of Metals*, Chapman & Hall, London (1953).
2. R. D. McCammon and H. M. Rosenberg, *Proc. Roy. Soc. (London)*, *A*, **242,** 203 (1957).
3. C. Crussard, R. Borione, J. Plateau, Y. Morillon, and F. Maratray, *J. Iron Steel Inst. (London)*, **183,** 146 (1956).
4. J. Plateau, G. Henry, and C. Crussard, *Rev. univ. mines*, **12,** 543 (1956).
5. J. Plateau, G. Henry, and C. Crussard, *Rev. mét.*, **54,** 200 (1957).
6. G. Henry, J. Plateau, and J. Philibert, *Compt. rend.*, **246,** 2753 (1958).
7. M. Weisz and R. Cazaud, *Rev. mét.*, **56,** 299 (1959).
8. J. B. Lean, J. Plateau, C. Bachet, and C. Crussard, *Compt. rend.*, **246,** 2845 (1958).
9. C. Crussard, unpublished results (1948).
10. J. Plateau, C. Crussard, J. Faguet, G. Henry, M. Weisz, G. Sertour, and R. Esquerre, *Rev. mét.*, **55,** 679 (1958).
11. M. Hempel, *Proceedings International Conference on Fatigue of Metals*, Institution of Mechanical Engineers, London, 543 (1957).
12. J. A. Kies, H. L. Smith, and G. R. Irwin, to be published in *Rev. mét.*, **56** (1959).
13. C. Crussard and B. Jaoul, *Rev. mét.*, **47,** 589 (1950).
14. C. Crussard, *Rev. mét.*, **50,** 687 (1953).

DISCUSSION

H. C. Rogers, *General Electric Company*. The evidence presented for the fracture process called "glide-plane decohesion" (formerly described by the authors[1,2] as "ductile cleavage") consists principally of the observation that, on the surfaces of steel fractures occurring in the transition region, one begins to note the appearance of curved facets that do not possess the river pattern present in the normal cleavage fracture of ferrite. In addition, similar facets are observed when the fracture takes place at a low temperature following a prestrain at a higher temperature. It seems very likely that these are merely normal cleavage planes which have been curved by the previous deformation, whether local or general. The absence of river patterns may well be a result of the high dislocation density in the prestrained material. In any case, the slip-plane decohesion is hardly verified. Such a proposal would have been more acceptable if the material did not cleave. In a material that does not cleave, however, as the authors have noted, there do exist regions in ductile fractures that intermingle with the remains of ruptured voids and are relatively flat. It has been our experience, however, that these regions are not what one could really call facets, that is, regions sharply bounded by grain boundaries. Our interpretation of such regions is that they are the remains of the sides of voids that have been smeared out by the shearing deformation that accompanies the failure of what has been termed a "void sheet." The fact that there is an increase in the percentage of the fracture surface that is covered by such smooth areas in "shear" fractures, as compared with "fibrous" fractures, might be attributed to the increased ratio of shearing stress to normal stress, with a consequent larger smearing out of the voids before they are pulled apart by the normal stresses.

It should be pointed out that this argument does not question the possibility of a glide-plane decohesion but merely questions the strength of the evidence produced so far in favor of it, since it may well be that the voids are nucleated by such a mechanism but on a finer scale. In the case of copper,[3] there is good evidence that the void growth occurs by the same mechanism that produces the final fracture, which gives the rippled appearance to the surface of the smeared-out void. It is less easy to rationalize such a rippled surface as the result of a simple glide-plane decohesion.

As a final point, it would be helpful to know whether the authors feel that decohesion along the slip plane is a necessary condition for void formation. Although they give this impression, this conclusion is not well supported by their observations that because these markings are sometimes

present in voids in materials does not mean that they will always be present and that similar rupture surfaces are formed in highly viscous materials, presumably by a cavitation process.

References

1. J. Plateau, G. Henry, and C. Crussard, *Rev. mét.*, **54**, 200 (1957).
2. C. Crussard, R. Borione, J. Plateau, Y. Morillon, and F. Maratray, *J. Iron Steel Inst. (London)*, **183**, 146 (1956).
3. H. C. Rogers, Discussion to paper by A. H. Cottrell, Chapter 2 of this volume.

F. A. McCLINTOCK, *Massachusetts Institute of Technology*. It is interesting to notice the similarity between the striations observed by the authors on steel under repeated stress and those that the writer has observed in static tensile testing of a single-notched, plane strain specimen of 99.995% aluminum. The striations were likewise perpendicular to the direction of the propagation of the crack front and independent of the grain structure. Rough steps were also observed perpendicular to the crack front, but festooning of the striations on these steps was not as pronounced. The scale of the striations was much coarser, but no explanation can be offered for their size, in view of the slow, steady deformation of the specimen.

In their discussion of the rounding off of microcracks, the authors state that high triaxial stresses favor multiple glide and climb or cross slip. While multiple glide that produced vacancies would be facilitated, how are climb and cross slip affected?

C. CRUSSARD, J. PLATEAU, R. TAMHANKAR, G. HENRY, AND D. LAJEUNESSE (AUTHORS' REPLY). Regarding Rogers' comments concerning the decohesion along glide planes, although we could not give evidence to support our interpretation, we think that it is warranted on the basis of the arguments that have been developed in our paper:

1. Absence of continuity between the appearance of brittle fracture, where the cleavage surface is covered by river patterns, and zones of glide decohesion.

2. Observation, on electroplated sections, of rupture facets inclined about 45° to the tensile stress on the same samples where "glide decohesions" are observed by microfractography.

3. Similarity between glide decohesion in unidirectional and in fatigue tests. In fatigue tests, these facets are known to occur along glide planes, and it is probable that this situation also occurs in unidirectional tests.

The rippled appearance mentioned by Rogers has also been observed by us on badly formed dimples in the case of quenched Al-Cu alloy. It may be related to the mechanism for cross slipping, as suggested by Honeycombe. Nevertheless, this rippling seems to be enhanced by an alternating stress, as in the case of striation observed on our fatigue rupture surfaces.

The observation made by McClintock is extremely interesting, and the striation he observes might be related to a process of successive slip and tearing, the slip occurring at some distance in front of the tip of the crack, where, as suggested by Orowan, dislocations may concentrate until the small isthmus of metal between this area and the tip of the crack is torn away. However, we think a better explanation is that the fracture is of a shear type, starting from the top of the crack and traveling along the glide zones, in which case one could expect these zones to operate in an alternate way.